Published in final edited form as:
J Mech Behav Biomed Mater. 2014 January ; 29: . doi:10.1016/j.jmbbm.2013.02.018.

Mechanical forces in cerebral cortical folding: A review of measurements and models

P.V. Bayly[a,*], **L.A. Taber**[b], and **C.D. Kroenke**[c]

[a]Department of Mechanical Engineering and Materials Science, 1 Brookings Drive, Saint Louis, MO 63130, United States

[b]Department of Biomedical Engineering, Washington University in Saint Louis, 1 Brookings Drive, Saint Louis, MO 63130, United States

[c]Advanced Imaging Research Center, Department of Behavioral Neuroscience, and Oregon National Primate Research Center, Oregon Health & Sciences University, 3181 S.W. Sam Jackson Park Rd., Portland, OR 97239-3098, United States

Abstract

Folding of the cerebral cortical surface is a critical process in human brain development, yet despite decades of indirect study and speculation the mechanics of the process remain incompletely understood. Leading hypotheses have focused on the roles of circumferential expansion of the cortex, radial growth, and internal tension in neuronal fibers (axons). In this article, we review advances in the mathematical modeling of growth and morphogenesis and new experimental data, which together promise to clarify the mechanical basis of cortical folding. Recent experimental studies have illuminated not only the fundamental cellular and molecular processes underlying cortical development, but also the stress state and mechanical behavior of the developing brain. The combination of mathematical modeling and biomechanical data provides a means to evaluate hypothesized mechanisms objectively and quantitatively, and to ensure that they are consistent with physical law, given plausible assumptions and reasonable parameter values.

1. Introduction

The folded shape of the human brain allows the cerebral cortex, the thin (2–4 mm) outer layer of neurons and their associated processes, to attain a very large surface area (~1600 cm^2) relative to brain volume (~1400 cm^3). Cortical folding, or gyrification, is critical to human brain development and function. Abnormal cortical folding has been associated with cognitive or emotional problems, including severe retardation, epilepsy (Pang et al., 2008), autism (Hardan et al., 2004; Nordahl et al., 2007) and schizophrenia (Csernansky et al., 2008a; Harris et al., 2004; Sallet et al., 2003). In humans, cortical folding normally occurs in utero, during the third trimester (Fig. 1).

Large mammals (cows, sheep, whales, dogs) and small carnivorous mammals (cats, raccoons, and ferrets) also have folded brains (Welker, 1990); although rats and mice do not. The ferret is a particularly convenient model in which to study folding because cortical folding occurs postnatally (Fig. 1), roughly between the 5th and 30th days after birth. The development of folds in the ferret brain was described in two seminal papers by Smart and McSherry (1986a, 1986b) who studied the evolution of gross anatomical features of the brain, as well as basic histological changes during this period. The developing ferret brain

*Corresponding author. Tel.: +1 314 935 6081. baylyp@seas.wustl.edu (P.V. Bayly).

has also been studied more recently using MR imaging (Barnette et al., 2009; Knutsen et al., 2012; Neal et al., 2007) and more advanced histological methods (Jespersen et al., 2012; Reillo et al., 2011).

Disturbances of cortical folding in humans are clinically important and offer clues to the underlying mechanisms of normal development (Manzini and Walsh, 2011; Pang et al., 2008; Pavone et al., 1993; Richman et al., 1973; Stewart et al., 1975). Outward, or convex, folds are known as *gyri* and inward folds are called *sulci. Lissencephaly* refers to the complete absence of folds, and is associated with greatly reduced numbers of cells in the cortex. *Polymicrogyria* involves numerous small, shallow cortical folds. *Pachygyria* is characterized by a relatively coarse folding pattern, with fewer and larger gyri.

Despite decades of intense study (Barron, 1950; Hofman, 1989; Le Gros Clark, 1945; Welker, 1990) and speculation, the mechanical basis of folding remains controversial. In subsequent sections of this review we briefly describe the basic neurobiology of cortical development, summarize pertinent experimental observations, and discuss the leading theories of folding mechanics.

2. Neurobiology of development

Brain tissue consists of two cell types. Neurons are responsible for conducting electrical impulses and participating in synaptic connections with other neurons, thereby determining the circuitry of the brain. Three primary morphological components of neurons are: the cell body, which contains the cell nucleus; dendrites, which are processes that receive and integrate information from other neurons; and the axon, which conducts electrical impulses from the cell body to other neurons. Glial cells are responsible for other brain functions, including structural roles in directing neuron migration during brain development, and ensheathing axons with myelin to facilitate neural impulse conduction. On the macroscopic scale, brain tissue can be divided into gray matter and white matter. Gray matter, which includes cerebral cortex, primarily consists of neuron cell bodies, dendrites, and synapses. White matter primarily consists of axons and myelin.

Although the timing of onset of cerebral cortical folding relative to the end of gestation varies considerably between species, this variance can primarily be attributed to interspecies differences in the lengths of gestation. With respect to other milestones of central nervous system development, the onset of cerebral cortical folding is consistent between species, and takes place after the majority of cerebral cortical neurons have been born and have completed migration from their sites of origin (cell layers at or near the surface of the lateral ventricle (Rakic, 1995)) to the nascent cerebral cortex, which is termed the cortical plate at its earliest stages of development.

Three notable events that occur simultaneously with cerebral cortical folding are: (i) dramatic expansion of the surface area of the cortex, (ii) morphological differentiation of neurons, which involves extension and branching of axonal and dendritic structures (Fig. 2), and (iii) growth of axon termini from the subplate (a developmentally-transient tissue zone that borders the cortex) into the cortical plate. After the conclusion of these three events, only subtle changes to the shape of the cerebral cortex take place.

Evidence that the process of cerebral cortical folding is linked to brain function underscores the importance of understanding its underlying biomechanics. Congenital brain defects such as lissencephaly, polymicrogyria, and pachygyria are associated with severe mental retardation (Manzini and Walsh, 2011; Pang et al., 2008; Pavone et al., 1993; Richman et al., 1973; Stewart et al., 1975). More subtle abnormalities in cortical folding observed in less severe neurological conditions provide further evidence that the mechanism that drives

cortical folding may be linked to the biological source of some neurodevelopmental disorders. In prematurely delivered human infants, cerebral cortical folding abnormalities have been observed, and premature birth is associated with subsequent behavioral and cognitive deficits that become apparent later in childhood (Dubois et al., 2008). Cortical folding abnormalities have also been identified in individuals with Williams syndrome (Van Essen et al., 2006b) and schizophrenia (Csernansky et al., 2008b; Harris et al., 2004; Sallet et al., 2003). In autistic individuals, anomalous cortical folding is observed when compared to age-matched controls (Hardan et al., 2004; Nordahl et al., 2007), and the effect on folding is related to the severity of the behavioral deficit (Nordahl et al., 2007). Collectively, these findings indicate that abnormalities in folding of the cerebral cortex may relate to alterations in brain function.

3. Experimental measurements and observations

The basic question concerning the mechanics of cortical folding is: what forces cause deformation? Is deformation driven by tensile stresses in the interior of gyri (Van Essen, 1997), by growth-driven, tangential compressive stresses in the outer layers of the cortex (Bayly et al., 2013; Richman et al., 1975; Xu et al., 2010), by heterogeneous outward radial growth (Smart and McSherry, 1986a, 1986b), or a combination of these mechanisms? In this section we discuss key measurements and observations that must be considered in developing models of folding.

3.1. Anatomical observations

Neuroanatomists have studied for decades the shape and size of the brain and its substructures in search of clues to the mechanics of folding. Anatomical findings are summarized in comprehensive reviews by Hofman (1989) and Welker (1990), as well as in landmark papers by Le Gros Clark (1945), Smart and McSherry (1986a, 1986b), Rakic (1988), and Van Essen (1997). Key observations include the following:

A. The thickness of the cortex is relatively consistent between species (Hofman, 1989). The mean thickness of the ferret cortex is approximately 1 mm while the mean thickness of the human cortex is approximately 3 mm (ratio of 1:3). The cortex is slightly thinner under the bases of sulci and thicker at the crests of gyri (Le Gros Clark, 1945). Inter-species variations in cortical surface area are disproportionately larger: the cortical surface area of the ferret is about 24 cm^2 and the human is 1600 cm^2 (a ratio of 1:70). Extensive comparisons between cortical parameters in different species are presented by Hofman (1989).

B. Some surgical interventions can affect folding patterns. Removing sub-cortical brain structures did not prevent cortical folding in the raccoon (Welker, 1990) and sheep (Barron, 1950) brain, though it influenced the shape of the folds (Barron, 1950; Welker, 1990). Lesions of the cortex itself affect folding locally, but also lead to anomalies at distant sites (Goldman and Galkin, 1978). Deprivation of visual input led to extra folds in the occipital lobes (visual cortex) of monkeys (Rakic, 1988).

C. Radial growth is heterogeneous—some sub-cortical layers expand outward to form the bases of gyri, while very little outward growth occurs under sulci (Smart and McSherry, 1986a) (Fig. 3). However, these anatomical observations do not clarify whether this heterogeneity in sub-cortical radial growth is the *cause* or the *result* of tangential expansion of the cortex.

3.2. Observations from cell biology and genetics

The generation of neurons, and their proper migration to the cortex can have a strong influence on its growth and ultimately, its final shape. Thus perturbations to the normal process of neuron proliferation in development can affect folding of the cerebral cortex. The ferret brain can be made lissencephalic by disrupting cell division, for example, by prenatal injection of the mitotic inhibitor methylazoxymethanol acetate (MAM). Further, folding can be induced in the typically lissencephalic mouse brain by genetic manipulations that disturb the regulation of the cell cycle in neural precursor cells (Chenn and Walsh, 2002) leading to excessive growth. Radially aligned glial cells provide a fibrous scaffold for migration. Reillo et al. (2011) have proposed that the existence of intermediate radial glial cells creates a fan-shaped, expanding network of radial glial fibers that enables rapid tangential expansion of the cortex in folded brains. In animals with smooth brains, these intermediate glia do not exist and the radial glial lattice does not expand at the cortex (Reillo et al., 2011).

3.3. Measurements from magnetic resonance imaging studies

Magnetic resonance imaging (MRI) allows noninvasive measurement of brain development. MRI can detect both macroscopic geometric changes and changes in cellular-level morphology, which can be inferred from diffusion tensor imaging (DTI) measurements. MRI studies of folding in the ferret brain performed by Neal et al. (2007), Barnette et al. (2009), Kroenke et al. (2009), and Knutsen et al. (2012) have characterized the temporal and spatial patterns of growth. These studies have established that folding of the ferret cerebral cortex occurs roughly between the 10th and 30th postnatal days (P10–P30), which precedes myelination of white matter (Knutsen et al., 2012; Neal et al., 2007).

Comparisons between DTI and MRI-derived measurements of surface area expansion in the ferret have shown a link between neuronal morphological differentiation and macroscopic changes. In the immature cerebral cortex, the simple radial organization of cellular processes gives rise to anisotropy in water diffusion; motion of water molecules is less restricted perpendicular to the cortical surface than it is in other directions. Such diffusion anisotropy can be measured by DTI (see Leigland and Kroenke, 2011 for a review), and quantified in terms of fractional anisotropy (FA) (Basser and Pierpaoli, 1996), a parameter that ranges from 0 (purely isotropic diffusion) to 1 (the limiting case of extreme diffusion anisotropy). In the ferret, cortical FA decreases exponentially from P10 through P30 due to cellular morphological differentiation (Fig. 4) (Kroenke et al., 2009; Leigland and Kroenke, 2011)). At the same time, the ferret cerebral cortex undergoes rapid expansion in surface area and accelerated folding (Knutsen et al., 2012). The rate of expansion of the isocortex is approximately 17 mm^2/day per hemisphere before P13 and 37 mm^2/day per hemisphere after P13 (Knutsen et al., 2012). Non-dimensional measures of average curvature ($\bar{K^*}$) and sulcal depth ($\bar{\Delta^*}$) increase concurrently with morphological differentiation (as revealed through the loss of cortical FA) (Fig. 4). The local curvature parameter $K^*=KL_c$, where $K=1/2(\kappa_1+\kappa_2)$ is the local mean principal curvature, and L_c is a characteristic length equal to the radius of the sphere with the same surface area, $L_c=\sqrt{A/4\pi}$. Sulcal depth, Δ, is the distance from a point on the cortical surface to a point on the convex hull; the non-dimensional value is normalized by the characteristic length: $\Delta^*=\Delta/L_c$. The global measures $\bar{K^*}$ and $\bar{\Delta^*}$ are calculated by averaging local non-dimensional curvature (K^*) and sulcal depth (Δ^*) over the cortical surface. For a sphere these parameters take the values $\bar{K^*}=1$ and $\bar{\Delta^*}=0$ (Knutsen et al., 2012).

Importantly, both the expansion of the cerebral cortical surface (Fig. 5a), as well as the loss of cortical FA due to morphological differentiation (Fig. 5b) occur non-uniformly with development. Spatial maps of areal expansion were estimated from measurements of $\Delta A=(A_2-A_1)/A_1$ for each small surface patch (initial area A_1, final area A_2; Fig. 5a). The

regional pattern of morphological development is highly similar to the pattern of local surface area expansion, which suggests a direct relationship between these processes. Thus it is plausible that morphological differentiation plays a key role in the mechanical processes that drive folding of the cerebral cortex.

3.4. Measurements of mechanical stress

Van Essen (1997) has proposed that *axonal tension* produces folding by drawing sides of gyri together. This hypothesis suggests three questions that can be answered by direct experimentation. (i) Can axons in vitro sustain mechanical tension? (ii) Are axons in the intact brain under tension? (iii) Does axonal tension act to draw the walls of gyri together?

Several studies by Heidemann and Buxbaum (1990, 1994) Chada et al. (1997), Dennerll et al. (1989) have addressed the first question. Dennerll et al. (1989) showed that neural fibers from embryonic chick peripheral neurons (dorsal root ganglia) in vitro can maintain tension. These sensory neurites demonstrated viscoelastic lengthening and towed growth during the application of tension, and active contraction to re-establish tension after the fiber was allowed to slacken. Neurites maintained levels of steady tension of 100–200 μ dynes (10–20 pN), and transient peak tension levels >500 μ dynes (>50 pN). Neural fibers from the brain itself also grew in vitro in response to applied tension, but maintained much lower levels of tension and did not re-establish tension after slackening (Chada et al., 1997).

Dissection experiments (Xu et al., 2009, 2010) convincingly showed that white matter in mammalian brains is under tension, including the white matter in the adult mouse brain (Xu et al., 2009) (Fig. 6) and in both mature and developing ferret brains (Xu et al., 2010) (Fig. 7). Incisions through cortical gray matter did not open, but cuts through white matter normal to the fiber direction opened, indicating stress along the fiber axis. The majority of axonal fibers in gyri project radially, and so the stress field within each gyrus appears to be dominated by tension in these radially-oriented fibers.

4. Models

In the following sections we describe recent or well-known models and evaluate them in terms of the experimental observations described above. Some of these models are based explicitly on mathematical equations that relate stresses to deformation. Other models are currently based on descriptive or intuitive arguments, or on scaling or geometrical relationships.

4.1. Axonal tension-driven folding

The axonal tension hypothesis (Van Essen, 1997) is illustrated schematically in Fig. 8a. This hypothesis, that axonal tension creates gyri, is attractive because it is consistent with efficient wiring—axons that connect related areas will draw them together, thus decreasing the total length of axonal connections. Disturbances in folding accompany alterations in axonal connectivity, as observed by Van Essen et al. (2006a) who analyzed cortical folding in subjects with a genetic disorder known as Williams syndrome. Rakic (1988) noted similar effects in the brains of monkeys with disrupted visual systems. However, in both cases the causality and mechanism are not clear. The axonal tension hypothesis is particularly interesting because tension can be measured in individual axons (Chada et al., 1997; Heidemann and Buxbaum, 1990, 1994; Joshi et al., 1985) as well as in tissue (Xu et al., 2009, 2010), as described above. However the hypothesis that the walls of gyri are drawn together by axonal tension is not consistent with observed patterns of stress in the ferret brain, which reflect tension along, not across, gyri (Xu et al., 2010) (Fig. 8b; see also Figs. 6 and 7).

4.2. Growth-driven folding

4.2.1. Buckling of stiff surface layers on elastic foundations—An influential study by Richman et al. (1975) points to *differential tangential growth*, in which outer layers grow tangentially at faster rates than inner layers of the brain, as the driving mechanism of cortical folding. In this study, the authors developed mathematically a hypothesis that had been discussed for many decades prior (see Le Gros Clark, 1945; Richman et al., 1975, and references therein). In the Richman model (Fig. 8c and d), tangential growth of the outermost cortical layer occurs at a greater rate than a second cortical layer, which overlies an elastic core. This differential growth produces compressive stress that leads to buckling of the cortical layers, modulated by the stiffness of the foundation. In terms of developmental neuroanatomy (see Bystron et al., 2008) the outer layers in this model comprise the cortical plate, and the foundation, or core, captures the aggregate mechanical behavior of subplate, intermediate zone, subventricular zone, ventricular zone, and all deeper internal brain structures. In the Richman model (Richman et al., 1975), increasing the material stiffness, or elastic modulus, of the foundation leads to shorter wavelengths of the buckled layer (cortex). The details of the analysis are not included in the paper (Richman et al., 1975), but the predictions correspond to the classic theory of the elastic buckling of a plate on an elastic foundation (Biot, 1965). However, the Richman model (Richman et al., 1975) relies on a large mismatch in the elastic moduli between the stiff outer layer and softer core to produce buckling patterns that approximate observed folds. In fact, experiments have indicated that the elastic modulus of the outer layer of cortex is not significantly different from that of inner regions of the brain (Chatelin et al., 2010; Prange and Margulies, 2002; van Dommelen et al., 2010).

More recent modeling work has extended the set of results for buckling of stiff elastic layers on softer continua. Hohlfeld and Mahadevan (2011) analyzed the surface instability in a strip of soft, hyperelastic, incompressible material with a thin, stiff, skin as it undergoes bending. This instability leads to furrows, or “sulci” that resemble cortical folds. Buckling of an elastic shell on an elastic foundation has also been used to explain the formation of ridges and whorls during fingerprint formation (Kucken and Newell, 2005) and the ridged or wrinkled skins of vegetables and fruits (Yin et al., 2008) (Fig. 9).

Some buckling models have been proposed which do not attempt to explicitly represent the physics of brain deformation, but instead rely on analogies to simpler behavior. A highly simplified, large-amplitude buckling model of cortical folding was presented by Raghavan et al. (1997). They represented the cortex as a thin elastic beam and predicted the buckled shape by minimizing an energy density function that consisted of the bending and stretching strain energy of the beam, skull constraints, and additional interaction terms that discouraged self-contact and looping. Nie et al. (2010 built a 3D model of cortical surface growth that mathematically describes the process of cortical expansion and bending. However their equations were not based on a physical model of the brain and were not intended to represent the true mechanics of deformation. Like Raghavan et al. (1997), Nie et al. (2010) used penalty terms to enforce constraints such as specific cranial volume and non-intersection of the cortical surface. Such terms are not required in the physically-based mechanical models described in the next section.

4.2.2. Elastic instability in growing continua—Rigorous models of growth in mechanical continua have been developed in the last two decades and applied to the understanding of development and morphogenesis. In particular the theory of multiplicative growth due to Rodriguez et al. (1994) has been widely used to model the development and growth of biological tissues including cardiovascular tissue (Alford and Taber, 2008; Goktepe et al., 2010; Lin and Taber, 1995; Ramasubramanian et al., 2006; Taber and

Chabert, 2002), brain (Filas et al., 2013; Xu et al., 2009, 2010; Varner et al., 2010), and skin (Zollner et al., 2012a, 2012b). This theory underlies several recent mathematical models of the generation of folds and creases, although few of these models directly address the question of cortical folding.

The basic equations are summarized in the following paragraphs, more details can be found in (Rodriguez et al., 1994) and subsequent references. Using standard continuum mechanics terminology, the location of a material element in the reference configuration is denoted as $\boldsymbol{X}$ and the corresponding location of the same element in the deformed configuration as $\boldsymbol{x}$. The deformation gradient tensor $\boldsymbol{F}=\partial\boldsymbol{x}/\partial\boldsymbol{X}$ is expressed as the product of a growth tensor, $\boldsymbol{G}$, and an elastic deformation gradient tensor, $\boldsymbol{F}^*$:

$$F=F^*\cdot G. \quad (1)$$

Biological tissue is often modeled as a hyperelastic material, so the Cauchy stress tensor, σ, depends directly on the elastic deformation according to the constitutive relationship

$$\sigma=J^{*-1}\boldsymbol{F}^*\cdot\frac{\partial W}{\partial \boldsymbol{F}^{*T}}. \quad (2)$$

where W is the strain energy density function for the material and $J^*=det\boldsymbol{F}^*$ is the volume ratio of the elastic deformation. Typically, incompressible or nearly-incompressible, isotropic constitutive behavior is assumed. The strain energy depends only on the elastic deformation, so that for example in a nearly-incompressible, neo-Hookean material model the material behavior is defined by

$$W=\frac{\mu}{2}(I_1^*J^{*-2/3}-3)+\frac{\kappa}{2}(J^*-1)^2 \quad (3)$$

The strain energy depends on J^* and on the first invariant (trace) of the elastic right Cauchy–Green deformation tensor, $I_1^*=tr\,\boldsymbol{C}^*$, where $\boldsymbol{C}^*=\boldsymbol{F}^{*T}\cdot\boldsymbol{F}^*$. The shear modulus, μ, and the bulk modulus $\kappa(\kappa\gg\mu)$ are the key material parameters. The growth tensor $\boldsymbol{G}$ may be specified as a function of time or location, or it may be assumed to depend on stress, providing a mechanism for mechanical coupling through growth.

Models of growth in elastic continua exhibit folding. Ben Amar and Goriely (2005) used this basic approach to analyze the incremental deformations of a growing, incompressible, hyperelastic, spherical shell. They showed that growth leads to elastic instability with buckling modes of different wavelengths depending on growth parameters, as well as on the thickness of the shell. In this analysis, growth is specified (i.e., it does not depend on the stress in the material). Both uniform (Ben Amar and Goriely, 2005) and differential (radially-varying (Goriely and Ben Amar, 2005)) circumferential growth affect buckling of hyperelastic shells in the presence of positive external pressure.

Dervaux and Ben Amar (2011) analyzed a continuum model of a growing, elastic ring surrounding a circular elastic core with different elastic modulus. From a linear stability analysis of the incremental equations they predict buckling with relatively short wavelength when the outer ring is softer than the core, and relatively long wavelength when the ring is stiffer than the core. Dervaux and Ben Amar (2008) have also used this approach to model the growth-induced deformations of thin shells. Dervaux et al. (2011) have developed an elegant experimental system that uses differentially-swelling gels to produce smooth buckled patterns and creases in rings (Fig. 10). Jin et al. (2011) have also demonstrated the

development of folds and creases in growing, soft hyperelastic rings and tubes subject to either an internal or external rigid constraint.

These continuum models of growth-induced elastic stability provide a plausible explanation for the occurrence of folds. The main questions surrounding these models are the selection of elastic parameters, and their effects on folding wavelength. As noted above, the modulus of the outer layer of the cortex is very similar to the modulus of underlying gray matter and white matter, so that variations in the wavelength of folding are not fully explained by elastic instability.

4.2.3. Viscoelastic instability in a model of stress-induced growth—The time scale of folding is long enough for the brain to grow significantly in response to stress; growth in interior layers could lead to relaxation of the stresses induced by growth of the outer cortical layer. Such behavior of the deeper layers would resemble the response of a viscoelastic material, specifically a Maxwell fluid. Theoretical predictions for compressive folding instabilities in viscoelastic media were developed by Biot (1957). Bayly et al. (2013) extended Biot's analysis to the situation in which compressive stress is due to tangential growth of a thin elastic plate with thickness h (the cortex), and the embedding medium grows in response to stress. According to this analysis, Bayly et al. (2013) predicted that the wavelength of folds, λ, (normalized by thickness h) will depend on the ratio $\Gamma_G = G_0/R_f$ (the ratio of cortical growth rate G_0 to the rate constant of sub-cortical stress inducted growth, R_f), and $\beta = \mu/\mu_f$, the ratio of the short-term elastic modulus of the outer layer of cortex (μ) to the average modulus of deeper layers (μ_f). Specifically they predicted that,

$$\frac{\lambda}{h} = 2\pi\left(\frac{\beta(\Gamma+1)}{3\Gamma}\right)^{1/3}, \quad (4)$$

where Γ is the largest positive real root of the polynomial equation,

$$\Gamma^5 - \frac{64}{9}\beta^2\Gamma_G{}^3(\Gamma^2+2\Gamma+1) = 0 \quad (5)$$

The stress-driven growth model not only produces reasonable predictions of folding patterns and stress distributions, but reflects the behavior of living brain tissue on these time scales. With similar stiffnesses in the cortex and interior regions of the brain, this model can explain both (i) variations in wavelength of folds and (ii) the stress fields observed in the developing brain. In this model, the cortical growth rate, relative to how quickly the core grows in response to stress, largely determines the wavelength of cortical folds. Two-dimensional simulations confirmed that more rapid cortical expansion generally leads to shorter wavelengths (Fig. 11). Simulated wavelengths also scale directly with cortical thickness, as predicted by Eq. (4). The initial shape before tangential cortical expansion, as well as spatial variations in tangential expansion itself, may also affect the final shape (Fig. 12).

4.2.4. Heterogeneities in radial expansion and circumferential growth—While growth-induced instability may underlie the formation of folds, it does not explain the consistent location of some large gyri and sulci. Two candidate mechanisms are identified for the formation of these consistent *primary* gyri. (i) Heterogeneous radial growth before the period of folding may set up small variations in initial conditions (shape, stiffness, or stress) that are amplified by tangential expansion of the cortex. We note that axonal tension, while not actively producing folds, may be an important feature of such an initial state. (ii) Tangential cortical expansion itself may be heterogeneous in both time and space, as

suggested in (Xu et al., 2010) (Fig. 13). Current experimental data do not disprove either of these possibilities. It is clear that the shape of the brain before folding is not perfectly smooth (Barnette et al., 2009; Neal et al., 2007; Smart and McSherry, 1986a, 1986b); we have also observed that on a coarse scale, cortical expansion is non-uniform (Knutsen et al., 2012).

4.3. Models based on geometry and scaling

Several investigators have made predictions regarding cortical folding without directly addressing the mechanical forces involved. Todd (1982) suggested that initial curvature determines the folding pattern, with sulci evolving from lines of minimal curvature. Though not based on a specific mechanical model, Todd's (1982) prediction is consistent with the effect of initial conditions in growth-driven folding models. Prothero and Sundsten (1984) use scaling arguments to predict cortical shape based strictly on the requirement for a "gyral window" large enough for white matter tracts to communicate with the neurons in each gyrus. Chklovskii et al. (2002) analyzed the volume of axonal white matter that would be optimal to connect all the neurons in cortical gray matter. More recently Herculano-Houzel et al. (2010), Mota and Herculano-Houzel (2012) have found consistent relationships between the volume and surface area of white matter and the number of cortical neurons. While these scaling models do not attempt to explain the mechanical forces that drive gyrogenesis, they provide valuable information on the neurobiological functions that must be achieved by the brain in its final form.

5. Discussion

Advances in the modeling and simulation of growing tissue, combined with new methods in biology, imaging, and mechanical measurement, have illuminated the mechanical forces that cause cortical folding. In particular, it is clear that a unique explanation cannot be determined from the kinematics of folding alone. More than one mechanical process can produce the changes in shape that occur during gyrogenesis. While axonal tension-driven models (Van Essen, 1997), and models in which the cortex is pushed outward by sub-cortical growth (Mota and Herculano-Houzel, 2012), may produce realistic shapes similar to the folded brain, geometric similarity is not sufficient evidence of the underlying hypotheses. For example, the predictions of tension-driven models are not consistent with the experimental observations of stress state described in Xu et al. (2010).

Tangential cortical expansion is clearly a key process in cortical folding, but it must be coupled with radial growth. Models based on elastic buckling, such as the model of an expanding plate on an elastic foundation, seem to rely on unrealistic differences in elastic moduli to produce observed folding patterns. The predictions of a stress-driven growth model (Bayly et al., 2013), using reasonable estimates of parameters from experimental studies (Chada et al., 1997; Knutsen et al., 2012) seem generally consistent with both observed folding patterns and observed stress distributions (Xu et al., 2010). If stress-dependent growth is the basic mechanism of folding, it is quite likely that the folding patterns produced are modulated by heterogeneities in radial growth, tangential growth, and the stress state before rapid cortical expansion begins.

5.1. Limitations and future work

Several of the theoretical studies use linear theory, or for other reasons focus on the mechanisms that govern only the initial formation and wavelengths of gyri. Closed-form solutions are likely to be obtained only in the small-deformation regime, but further numerical studies should explore the large-deformation, post-buckled behavior of these models. Such studies will need to exploit more advanced simulation techniques to achieve

convergence and accuracy under these conditions. The domains of current physically-based simulations are simple; the extension of modeling and simulation to the full 3D case with realistic initial shapes (as in Nie et al. (2010)) is clearly warranted.

The experimental studies described here should also be interpreted cautiously. Experimental measurements of stress in the developing brain have been performed in brain slices, so the stress field has been changed by the release of any stresses on the plane of the cut. MR imaging measurements of spatial variations of growth would be improved by following a dense set of markers or landmarks. For example, surface strain in the embryonic chick brain has been measured by tracking displacements of beads attached to the surface (Filas et al., 2008). Reliable measurements of the mechanical properties of brain tissue as it develops remain difficult to obtain; estimates of properties obtained via indentation (Xu et al., 2010) are subject to the limitations and assumptions inherent in the technique.

6. Conclusions

The combination of quantitative, physically-meaningful, mathematical models and direct measurements of growth kinematics, tissue stresses, and brain material properties has provided new insight into the mechanics of cortical folding. The evidence suggests that the cortical folding process is driven by tangential expansion of the cortex and stress-induced growth of sub-cortical regions, modulated by initial shape and stress before the period of gyrogenesis.

Acknowledgments

Funding from NIH grant R01 NS070918 (Taber), R21 EB005834 (Bayly), NSF grant DMS0540701 (Taber) and R01 NS070022 (Kroenke) is gratefully acknowledged.

References

Alford PW, Taber LA. Computational study of growth and remodelling in the aortic arch. Computer Methods in Biomechanics and Biomedical Engineering. 2008; 11:525–538. [PubMed: 18792831]

Barnette AR, Neil JJ, Kroenke CD, Griffith JL, Epstein AA, Bayly PV, Knutsen AK, Inder TE. Characterization of brain development in the ferret via MRI. Pediatric Research. 2009; 66:80–84. [PubMed: 19287340]

Barron DH. An experimental analysis of some factors involved in the development of the fissure pattern of the cerebral cortex. Journal of Experimental Zoology. 1950; 113:553–581.

Basser PJ, Pierpaoli C. Microstructural and physiological features of tissues elucidated by quantitative-diffusion-tensor MRI. Journal of Magnetic Resonance, Series B. 1996; 111:209–219. [PubMed: 8661285]

Bayly PV, Okamoto RJ, Xu G, Shi Y, Taber LA. A cortical folding model incorporating stress-dependent growth explains gyral wavelengths and stress patterns in the developing brain. Physical Biology. 2013; 10 (1):016005. [PubMed: 23357794]

Ben Amar M, Goriely A. Growth and instability in elastic tissues. Journal of the Mechanics and Physics of Solids. 2005; 53:2284–2319.

Biot MA. Folding instability of a layered viscoelastic medium under compression. Proceedings of the Royal Society of London—Series A: Mathematical, Physical and Engineering Sciences. 1957; 242:444–454.

Biot, MA. Mechanics of Incremental Deformations; Theory of Elasticity and Viscoelasticity of Initially Stressed Solids and Fluids, Including Thermodynamic Foundations and Applications to Finite Strain. Wiley; New York: 1965.

Bystron I, Blakemore C, Rakic P. Development of the human cerebral cortex: Boulder Committee revisited. Nature Reviews Neuroscience. 2008; 9:110–122.

Chada S, Lamoureux P, Buxbaum RE, Heidemann SR. Cytomechanics of neurite outgrowth from chick brain neurons. Journal of Cell Science. 1997; 110 (Pt 10):1179–1186. [PubMed: 9191042]

Chatelin S, Constantinesco A, Willinger R. Fifty years of brain tissue mechanical testing: from in vitro to in vivo investigations. Biorheology. 2010; 47:255–276. [PubMed: 21403381]

Chenn A, Walsh CA. Regulation of cerebral cortical size by control of cell cycle exit in neural precursors. Science. 2002; 297:365–369. [PubMed: 12130776]

Chklovskii DB, Schikorski T, Stevens CF. Wiring optimization in cortical circuits. Neuron. 2002; 34:341–347. [PubMed: 11988166]

Csernansky JG, Gillespie SK, Dierker DL, Anticevic A, Wang L, Barch DM, Van Essen DC. Symmetric abnormalities in sulcal patterning in schizophrenia. NeuroImage. 2008a; 43:440–446. [PubMed: 18707008]

Csernansky JG, Gillespie SK, Dierker DL, Anticevic A, Wang L, Barch DM, Van Essen DC. Symmetric abnormalities in sulcal patterning in schizophrenia. NeuroImage. 2008b; 43:440–446. [PubMed: 18707008]

Dennerll TJ, Lamoureux P, Buxbaum RE, Heidemann SR. The cytomechanics of axonal elongation and retraction. Journal of Cell Biology. 1989; 109:3073–3083. [PubMed: 2592415]

Dervaux J, Ben Amar M. Morphogenesis of growing soft tissues. Physical Review Letters. 2008:101.

Dervaux J, Ben Amar M. Buckling condensation in constrained growth. Journal of the Mechanics and Physics of Solids. 2011; 59:538–560.

Dervaux J, Couder Y, Guedeau-Boudeville MA, Ben Amar M. Shape transition in artificial tumors: from smooth buckles to singular creases. Physical Review Letters. 2011:107.

Dubois J, Benders M, Borradori-Tolsa C, Cachia A, Lazeyras F, Ha-Vinh Leuchter R, Sizonenko SV, Warfield SK, Mangin JF, Huppi PS. Primary cortical folding in the human newborn: an early marker of later functional development. Brain. 2008; 131:2028–2041. [PubMed: 18587151]

Filas BA, Knutsen AK, Bayly PV, Taber LA. A new method for measuring deformation of folding surfaces during morphogenesis. Journal of Biomechanical Engineering. 2008; 130:061010. [PubMed: 19045539]

Filas, BA.; Xu, G.; Taber, LA. Mechanisms of brain morphogenesis. In: Holzapfel, GA.; Kuhl, E., editors. Computer Models in Biomechanics. Springer; New York: 2013. p. 337-349.

Goktepe S, Abilez OJ, Parker KK, Kuhl E. A multiscale model for eccentric and concentric cardiac growth through sarcomerogenesis. Journal of Theoretical Biology. 2010; 265:433–442. [PubMed: 20447409]

Goldman PS, Galkin TW. Prenatal removal of frontal association cortex in the fetal rhesus monkey: anatomical and functional consequences in postnatal life. Brain Research. 1978; 152:451–485. [PubMed: 99206]

Goriely A, Ben Amar M. Differential growth and instability in elastic shells. Physical Review Letters. 2005:94.

Hardan AY, Jou RJ, Keshavan MS, Varma R, Minshew NJ. Increased frontal cortical folding in autism: a preliminary MRI study. Psychiatric Research. 2004; 131:263–268.

Harris JM, Whalley H, Yates S, Miller P, Johnstone EC, Lawrie SM. Abnormal cortical folding in high-risk individuals: a predictor of the development of schizophrenia? Biological Psychiatry. 2004; 56:182–189. [PubMed: 15271587]

Heidemann SR, Buxbaum RE. Tension as a regulator and integrator of axonal growth. Cell Motility and the Cytoskeleton. 1990; 17:6–10. [PubMed: 2225090]

Heidemann SR, Buxbaum RE. Mechanical tension as a regulator of axonal development. Neurotoxicology. 1994; 15:95–107. [PubMed: 8090366]

Herculano-Houzel S, Mota B, Wong P, Kaas JH. Connectivity-driven white matter scaling and folding in primate cerebral cortex. Proceedings of the National Academy of Sciences of the United States of America. 2010; 107:19008–19013. [PubMed: 20956290]

Hofman MA. On the evolution and geometry of the brain in mammals. Progress in Neurobiology. 1989; 32:137–158. [PubMed: 2645619]

Hohlfeld E, Mahadevan L. Unfolding the sulcus. Physical Review Letters. 2011:106.

Jespersen SN, Leigland LA, Cornea A, Kroenke CD. Determination of axonal and dendritic orientation distributions within the developing cerebral cortex by diffusion tensor imaging. IEEE Transactions of Medical Imaging. 2012; 31:16–32.

Jin L, Cai S, Suo Z. Creases in soft tissue generated by growth. EPL (Europhysics Letters). 2011; 95:64002.

Joshi HC, Chu D, Buxbaum RE, Heidemann SR. Tension and compression in the cytoskeleton of PC 12 neurites. Journal of Cell Biology. 1985; 101:697–705. [PubMed: 2863274]

Knutsen AK, Kroenke CD, Chang YV, Taber LA, Bayly PV. Spatial and temporal variations of cortical growth during gyrogenesis in the developing ferret brain. Cerebral Cortex. 2012

Kroenke CD, Taber EN, Leigland LA, Knutsen AK, Bayly PV. Regional patterns of cerebral cortical differentiation determined by diffusion tensor MRI. Cerebral Cortex. 2009; 19:2916–2929. [PubMed: 19363145]

Kucken M, Newell AC. Fingerprint formation. Journal of Theoretical Biology. 2005; 235:71–83. [PubMed: 15833314]

Le Gros Clark, WE. Deformation patterns in the cerebral cortex. In: Le Gros Clark, WE.; Medawar, PB., editors. Essays on Growth and Form. Oxford University Press; London: 1945. p. 1-22.

Leigland LA, Kroenke CD. A comparative analysis of cellular morphological differentiation within the cerebral cortex using diffusion tensor imaging. Neuromethods. 2011; 50:329–351.

Lin IE, Taber LA. A model for stress-induced growth in the developing heart. Journal of Biomechanical Engineering. 1995; 117:343–349. [PubMed: 8618388]

Manzini MC, Walsh CA. What disorders of cortical development tell us about the cortex: one plus one does not always make two. Current Opinion in Genetics and Development. 2011; 21:333–339. [PubMed: 21288712]

Mota B, Herculano-Houzel S. How the cortex gets its folds: an inside-out, connectivity-driven model for the scaling of mammalian cortical folding. Frontiers in. Neuroanatomy. 2012; 6:3.

Neal J, Takahashi M, Silva M, Tiao G, Walsh CA, Sheen VL. Insights into the gyrification of developing ferret brain by magnetic resonance imaging. Journal of Anatomy. 2007; 210:66–77. [PubMed: 17229284]

Nie J, Guo L, Li G, Faraco C, Stephen Miller L, Liu T. A computational model of cerebral cortex folding. Journal of Theoretical Biology i. 2010; 264:467–478.

Nordahl CW, Dierker D, Mostafavi I, Schumann CM, Rivera SM, Amaral DG, Van Essen DC. Cortical folding abnormalities in autism revealed by surface-based morphometry. Journal of Neuroscience. 2007; 27:11725–11735. [PubMed: 17959814]

Pang T, Atefy R, Sheen V. Malformations of cortical development. Neurologist. 2008; 14:181–191. [PubMed: 18469675]

Pavone L, Rizzo R, Dobyns WB. Clinical manifestations and evaluation of isolated lissencephaly. Child's Nervous System. 1993; 9:387–390.

Prange MT, Margulies SS. Regional, directional, and age-dependent properties of the brain undergoing large deformation. Journal of Biomechanical Engineering. 2002; 124:244–252. [PubMed: 12002135]

Prothero JW, Sundsten JW. Folding of the cerebral-ortex cortex in mammals—a scaling model. Brain Behavior and Evolution. 1984; 24:152–167.

Raghavan R, Lawton W, Ranjan SR, Viswanathan RR. A continuum mechanics-based model for cortical growth. Journal of Theoretical Biology. 1997; 187:285–296.

Rakic P. Specification of cerebral cortical areas. Science. 1988; 241:170–176. [PubMed: 3291116]

Rakic P. A small step for the cell, a giant leap for mankind: a hypothesis of neocortical expansion during evolution. Trends in Neurosciences. 1995; 18:383–388. [PubMed: 7482803]

Ramasubramanian A, Latacha KS, Benjamin JM, Voronov DA, Ravi A, Taber LA. Computational model for early cardiac looping. Annales of Biomedical Engineering. 2006; 34:1655–1669.

Reillo I, De Juan Romero C, Garcia-Cabezas MA, Borrell V. A role for intermediate radial glia in the tangential expansion of the mammalian cerebral cortex. Cerebral Cortex. 2011; 21:1674–1694. [PubMed: 21127018]

Richman DP, Stewart RM, Caviness VS. Microgyria, lissencephaly, and neuron migration to cerebral-cortex -architectonic approach. Neurology. 1973; 23:413.

Richman DP, Stewart RM, Hutchinson JW, Caviness VS. Mechanical model of brain convolutional development. Science. 1975; 189:18–21. [PubMed: 1135626]

Rodriguez EK, Hoger A, McCulloch AD. Stress-dependent finite growth in soft elastic tissues. Journal of Biomechanics. 1994; 27:455–467. [PubMed: 8188726]

Sallet PC, Elkis H, Alves TM, Oliveira JR, Sassi E, Campi De Castro C, Busatto GF, Gattaz WF. Reduced cortical folding in schizophrenia: an MRI morphometric study. American Journal of Psychiatry. 2003; 160:1606–1613. [PubMed: 12944334]

Smart IH, McSherry GM. Gyrus formation in the cerebral cortex in the ferret. I. Description of the external changes. Journal of Anatomy. 1986a; 146:141–152. [PubMed: 3693054]

Smart IH, McSherry GM. Gyrus formation in the cerebral cortex of the ferret. II. Description of the internal histological changes. Journal of Anatomy. 1986b; 147:27–43. [PubMed: 3693076]

Stewart RM, Caviness VS, Richman DP. Lissencephaly and pachygyria—architectonic and topographical analysis. Acta Neuropathologica. 1975; 31:1–12. [PubMed: 1121923]

Taber LA, Chabert S. Theoretical and experimental study of growth and remodeling in the developing heart. Biomechanics and Modeling in Mechanobiology. 2002; 1:29–43. [PubMed: 14586705]

Todd PH. A geometric model for the cortical folding pattern of simple folded brains. Journal of Theoretical Biology. 1982; 97:529–538. [PubMed: 6813602]

van Dommelen JA, van der Sande TP, Hrapko M, Peters GW. Mechanical properties of brain tissue by indentation: interregional variation. Journal of the Mechanical Behavior of Biomedical Materials. 2010; 3:158–166. [PubMed: 20129415]

Van Essen DC. A tension-based theory of morphogenesis and compact wiring in the central nervous system. Nature. 1997; 385:313–318. [PubMed: 9002514]

Van Essen DC, Dierker D, Snyder AZ, Raichle ME, Reiss AL, Korenberg J. Symmetry of cortical folding abnormalities in Williams syndrome revealed by surface-based analyses. Journal of Neuroscience. 2006a; 26:5470–5483. [PubMed: 16707799]

Van Essen DC, Dierker DL, Snyder AZ, Raichle ME, Reiss AL, Korenberg J. Symmetry of cortical folding abnormalities in Williams syndrome revealed by surface-based analyses. Journal of Neuroscience. 2006b; 26:5470–5483. [PubMed: 16707799]

Varner VD, Voronov DA, Taber LA. Mechanics of head fold formation: investigating tissue-level forces during early development. Development. 2010; 37:3801–3811. [PubMed: 20929950]

Welker, W. Why does the cortex fissure and fold: a review of determinants of gyri and sulci. In: Jones, EG.; Peters, A., editors. Cerebral Cortex: Comparative Structure and Evolution of Cerebral Cortex. Plenum Press; New York: 1990. p. 3-136.

Xu G, Bayly PV, Taber LA. Residual stress in the adult mouse brain. Biomechanics and Modeling in Mechanobiology. 2009; 8:253–262. [PubMed: 18651186]

Xu G, Knutsen AK, Dikranian K, Kroenke CD, Bayly PV, Taber LA. Axons pull on the brain, but tension does not drive cortical folding. Journal of Biomechanical Engineering. 2010; 132:071013. [PubMed: 20590291]

Yin J, Cao Z, Li C, Sheinman I, Chen X. Stress-driven buckling patterns in spheroidal core/shell structures. Proceedings of the National Academy of Sciences of the United States of America. 2008; 105:19132–19135. [PubMed: 19036924]

Zervas M, Walkley SU. Ferret pyramidal cell dendritogenesis: changes in morphology and ganglioside expression during cortical development. Journal of Comparative Neurology. 1999; 413:429–448. [PubMed: 10502250]

Zollner AM, Buganza Tepole A, Gosain AK, Kuhl E. Growing skin: tissue expansion in pediatric forehead reconstruction. Biomechanics and Modeling in Mechanobiology. 2012a; 11:855–867. [PubMed: 22052000]

Zollner AM, Buganza Tepole A, Kuhl E. On the biomechanics and mechanobiology of growing skin. Journal of Theoretical Biology. 2012b; 297:166–175. [PubMed: 22227432]

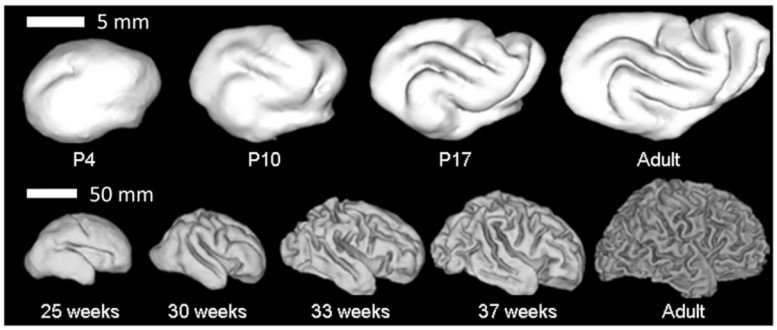

Fig. 1.

Surface representations obtained from MR images of (A) ferret brains at postnatal day 4, 10, 17, and at maturity, and (B) human brains at 25, 30, 33, and 39 weeks gestation and in the adult. Reproduced with permission from Barnette et al. (2009).

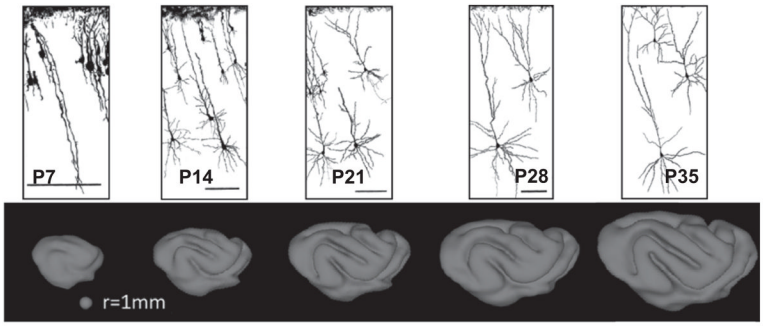

Fig. 2.

Neuronal differentiation and arborization coincide with the period of cerebral cortical folding. In the ferret, both morphological differentiation and folding occurs during the first five weeks of life. Neural traces are from Zervas and Walkley (1999) and are reproduced with permission.

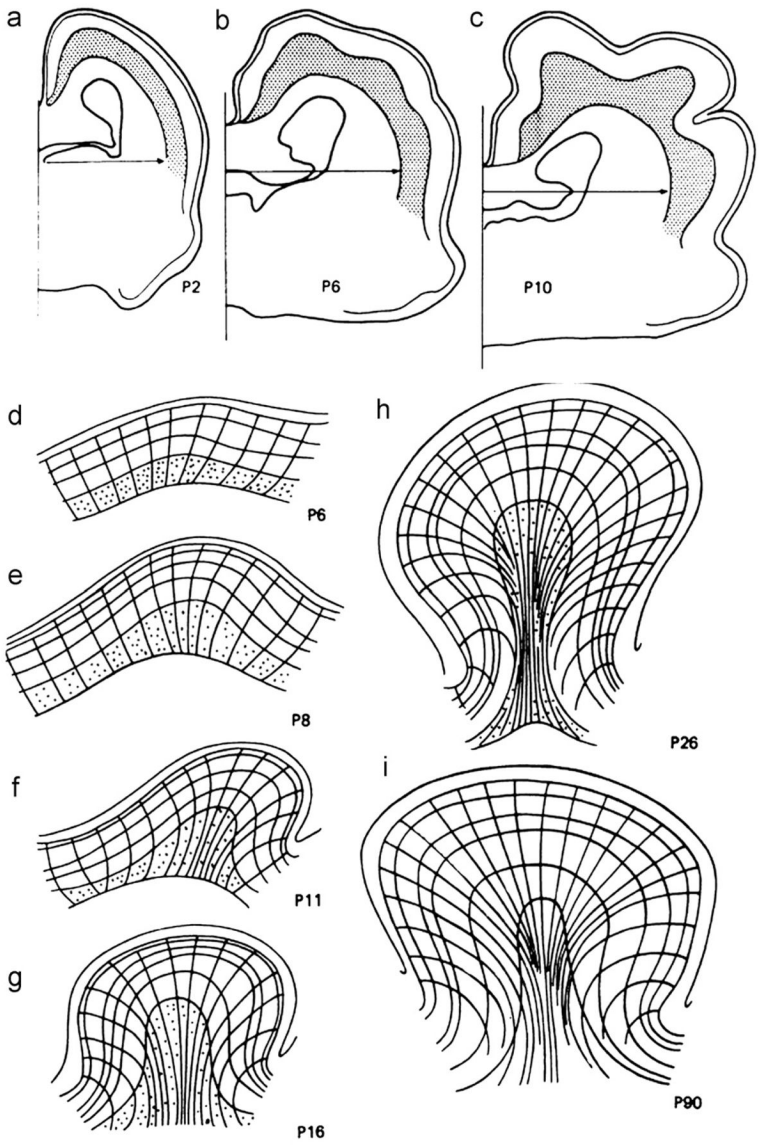

Fig. 3.

(a) Coronal sections of ferret brains fixed at 2, 6, and 10 days after birth (P2, P6, and P10). Reproduced with permission from Smart and McSherry (1986a). (b) Line drawings of tissue deformations during folding, from Smart and McSherry (1986b). Lines show radial tissue lines and layers in the tangentially expanding cortex; stippling shows neurons in the subplate (the layer immediately below the cortical plate). Reproduced with permission from Smart and McSherry,(1986b).

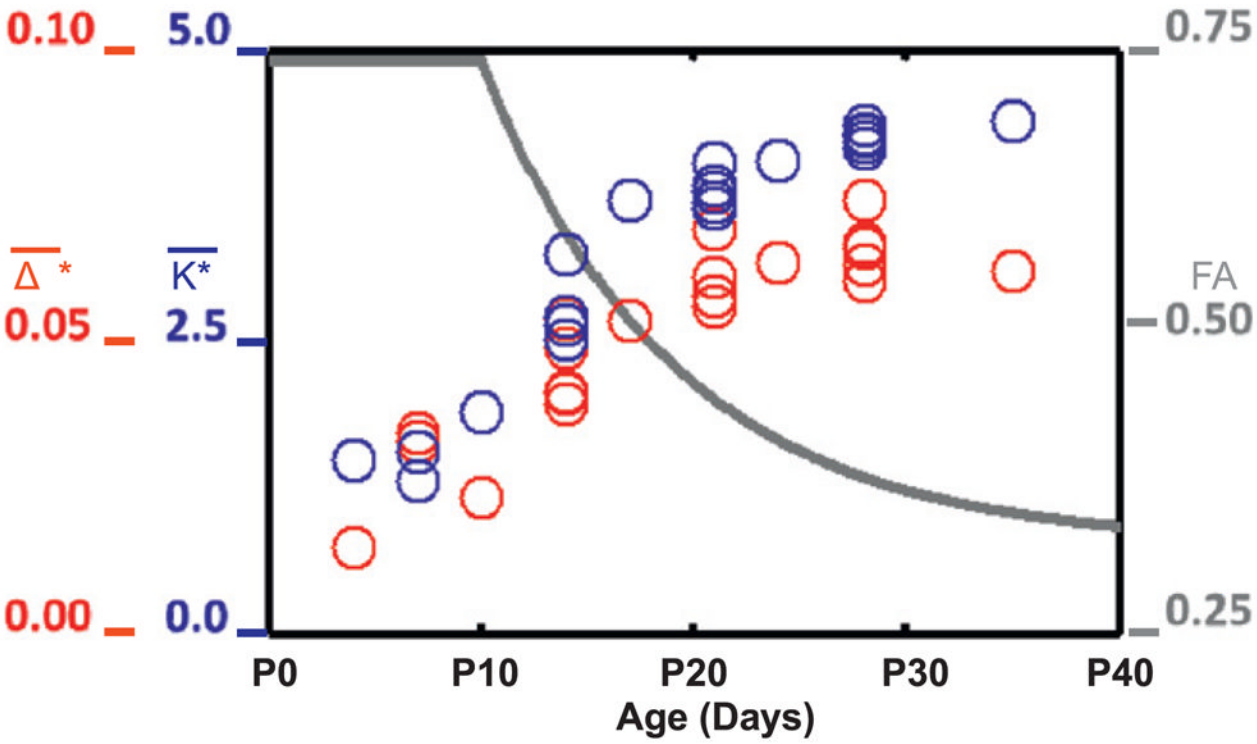

Fig. 4.

Fractional anisotropy of the diffusion tensor (measured by diffusion-weighted MR imaging) decreases during folding, as normalized mean curvature ($\bar{K^*}$) and normalized sulcal depth ($\bar{\Delta^*}$) increase. FA, $\bar{K^*}$ and $\bar{\Delta^*}$ are all dimensionless. Adapted with permission from Knutsen et al. (2012).

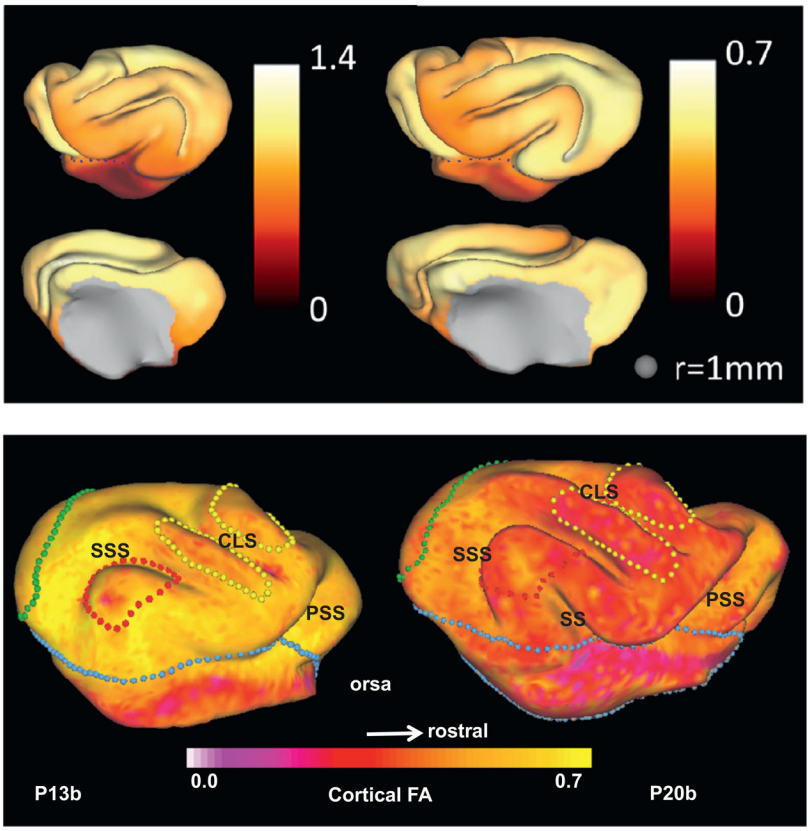

Fig. 5.

(a) Maps of local relative cortical growth, $\Delta A = (A_2 A_1)/A_1$ from P14 to P21 (left) and P21 to P28 (right) in the left hemisphere of one ferret. While the isocortex expands at a roughly constant rate after about P13, relative cortical growth is larger from P14 to P21 because cortical growth represents the change in local surface area relative to the initial local surface area. Growth was not calculated on the medial wall, which is shown in gray. Reproduced with permission from Knutsen et al. (2012). (b) Regional variations of cortical fractional anisotropy (FA) in the developing ferret brain. FA decreases with age over the first postnatal month (Kroenke et al., 2009). Here, cortical FA is projected onto P13b and P20b ferret brain cortical surface models, respectively. Boundaries between important cortical regions are marked by color-coded spheres on each surface: the isocortical/allocortical boundary (light blue); primary visual cortex (green); auditory cortex (red) and somatosensory area (yellow). Adapted with permission from Kroenke et al. (2009). (For interpretation of the references to color in this figure legend, the reader is referred to the web version of this article.)

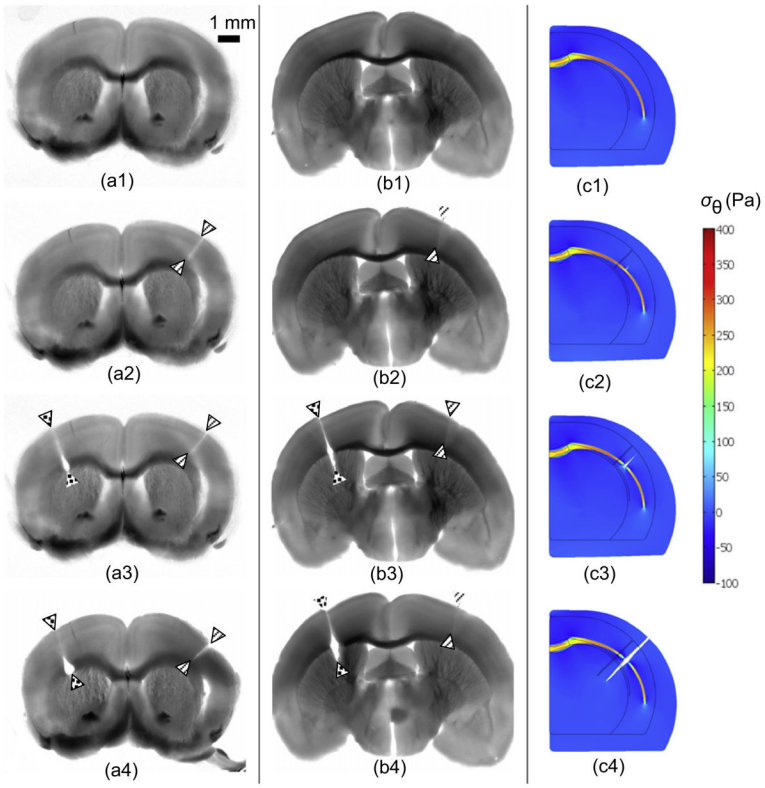

Fig. 6.

Micro-dissection study of stress in a coronal slice of an adult mouse brain. (a1, b1) Brain section before dissection (1 mm thick, obtained by vibratome immediately after sacrifice). (a2, b2) One radial cut (solid arrowheads) was made only through the cortical gray matter, and did not open. (a3, b3) A second radial cut (open arrowheads) was made through the underlying white matter (a3) or into the interior gray matter (b3). The cut opened at the site of the white matter tract. (a4, b4). (c1–c4) Normalized circumferential stress (σ_θ^*) distribution in finite element models of the dissection experiments (μ^*=0.5, λ_g^*=1.3). Following imposed growth, gray matter is in compression and white matter is in tension. Simulated radial cuts were made into cortical gray matter (c2), white matter (c3), or deep gray matter (c4), respectively. Reproduced with permission from Xu et al. (2009).

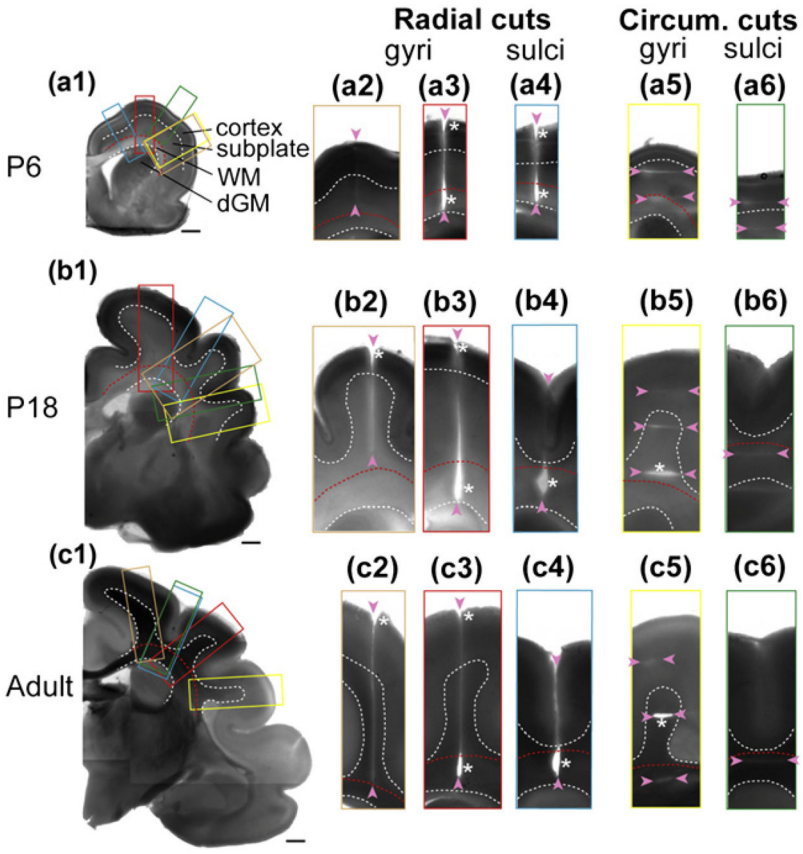

Fig. 7.

Microdissection study of the ferret brain before, during, and after the period of folding. (a1–c1) Coronal brain sections at postnatal day (P) 6, 18, and adult. Dashed curves outline the boundaries between cortex, subplate, subcortical white matter (WM), and deep grey matter (dGM). Scale bars represent 1 mm. Color-coded rectangles indicate the regions shown in the close-ups to the right of each section. Cuts of various depths (indicated by pairs of arrowheads) are made either radially (a2–a4, b2–b4, and c2–c4) or circumferentially (a5–a6, b5–b6, and c5–c6) on developing gyri and sulci as marked. Asterisks indicate significant openings. Reproduced with permission from Xu et al. (2010).

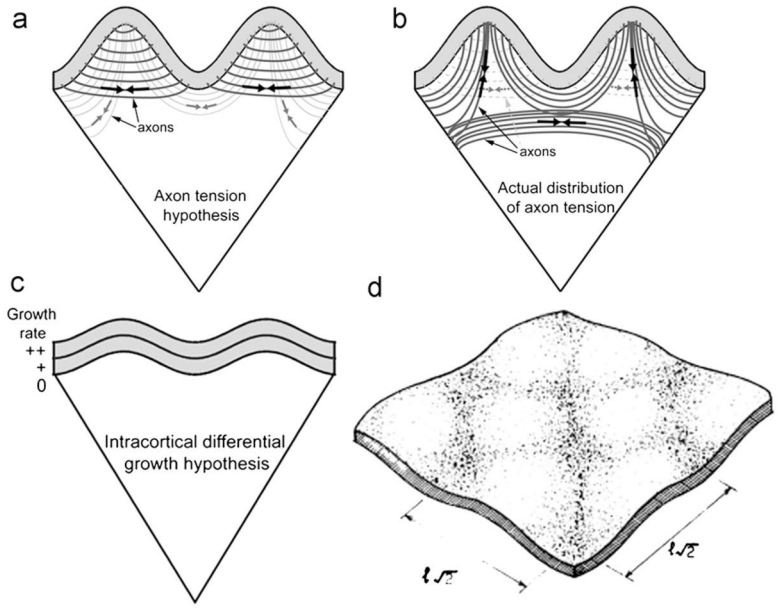

Fig. 8.

(a) A schematic representation of the *axonal tension hypothesis* of cortical folding (Van Essen, 1997). Tension (black arrows) in axons that connect two cortical regions is hypothesized to pull them closer to each other, forming an outward fold. Inward folds are hypothesized to form between weakly interconnected cortical regions (grey arrows). Adapted with permission from Xu et al. (2010) following Van Essen (1997). (b) Actual distributions of axon tension based on dissection and histology data (Xu et al., 2010). Axons are under tension (black arrows). Tension is manifested circumferentially in the subcortical white matter tract and radially in the subplate or the cores of outward folds (apparent after P18). Circumferential tension (grey arrows) was not detected between the walls of outward folds. Adapted with permission from Xu et al. (2010). (c) Intracortical *differential tangential growth* model due to Richman et al. (1975). Brain cortex is roughly divided into two layers with the outer layer growing faster (indicated by "++") than the inner layer ("+"). All other underlying tissue is treated as a softer elastic foundation without any growth. Adapted with permission from Richman et al. (1975) and Xu et al. (2010). (d) This differential growth model predicts elastic buckling of the outer layer. Reproduced with permission from Richman et al. (1975). (For interpretation of the references to color in this figure legend, the reader is referred to the web version of this article.)

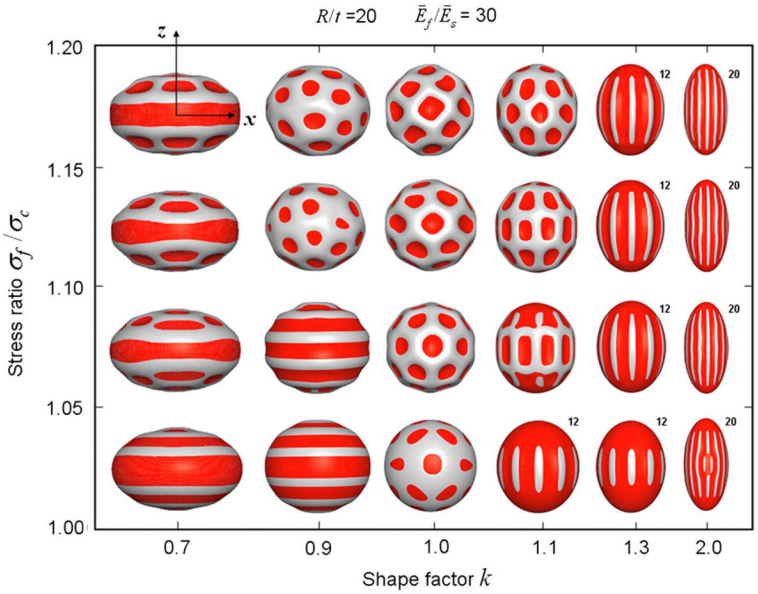

Fig. 9.

Buckling deformation maps of stiff-shelled spheroids with equatorial radius a, polar radius b, and shell thickness t, from Yin et al. (2008). The radius of curvature at the pole is $R=a^2/b$ and the shape factor $k=a/b$. Deformations of the outer shell are shown as shape factor k and ratio of stress in the film (shell) to critical buckling stress (σ_f/σ_c) are varied. The radius/thickness ratio R/t =20 and the modulus ratio between film and substrate E_f/E_s = 30 are both held constant. The amplitude of the mode in each image is arbitrary; the color red indicates relatively concave regions. Reproduced with permission from Yin et al. (2008). (For interpretation of the references to color in this figure legend, the reader is referred to the web version of this article.)

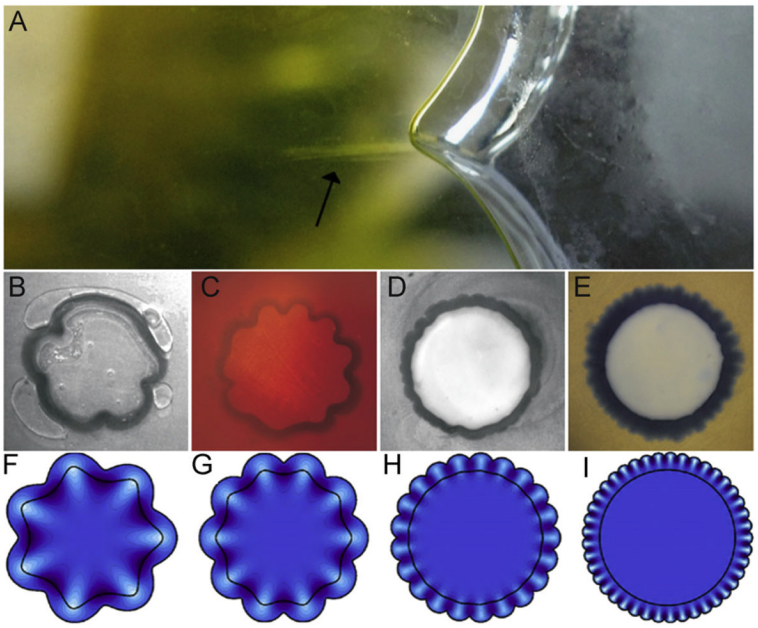

Fig. 10.

(A) A cusped structure representative of folding instability in a differentially swelling gel specimen (Dervaux et al., 2011). The outer ring (width H) swells while the inner disk (radius A) does not. (B)–(E) Experimental samples with ratios of ring width/internal disk radius ratio $H/A \approx 0.13$. The ratio of shear modulus in the disk to shear modulus in the ring increases from left to right: 0.25, 0.5, 1, 6). (F)–(I) Corresponding theoretical predictions. Reproduced with permission from Dervaux et al. (2011).

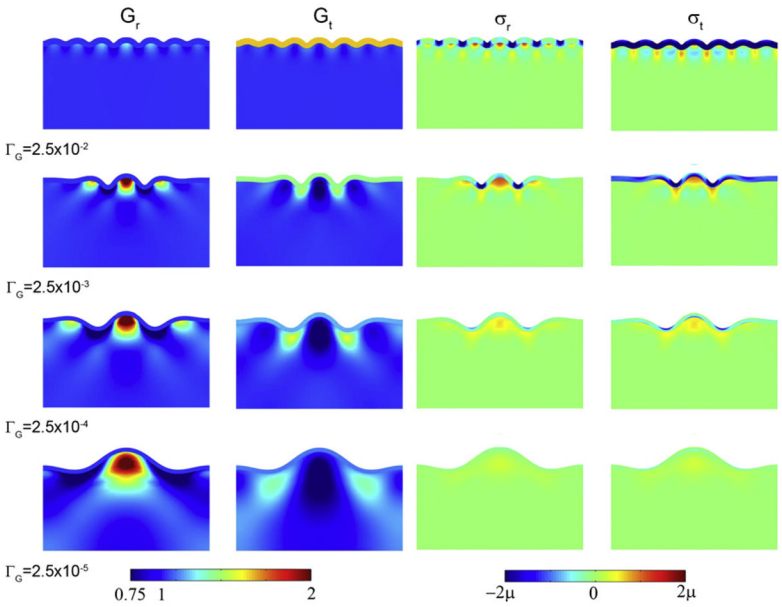

Fig. 11.

Effects of cortical growth rate on wavelength, subcortical growth, and stress in a 2-D model of cortical folding. In this model folding is driven by tangential growth of a single outer layer, accompanied by stress-driven radial and tangential growth in the foundation (Bayly et al., 2013). The elastic shear modulus is the same in both regions. Each column contains spatial maps of a different variable superimposed on the deformed geometry: radial growth G_r; tangential growth G_t; radial stress σ_r; tangential stress σ_t. Each row corresponds to a different scaled cortical growth rate. (Row 1)Relative growth rate $\Gamma_G = 2.5 \times 10^{-2}$, at scaled time τ=0.060; (Row 2) $\Gamma_G = 2.5 \times 10^{-3}$, at τ=0.035; (Row 3) $\Gamma_G = 2.5 \times 10^{-4}$, at τ=0.014; (Row 4) $\tau = 2.5 \times 10^{-5}$, at τ =0.08. Reproduced with permission from Bayly et al. (2013).

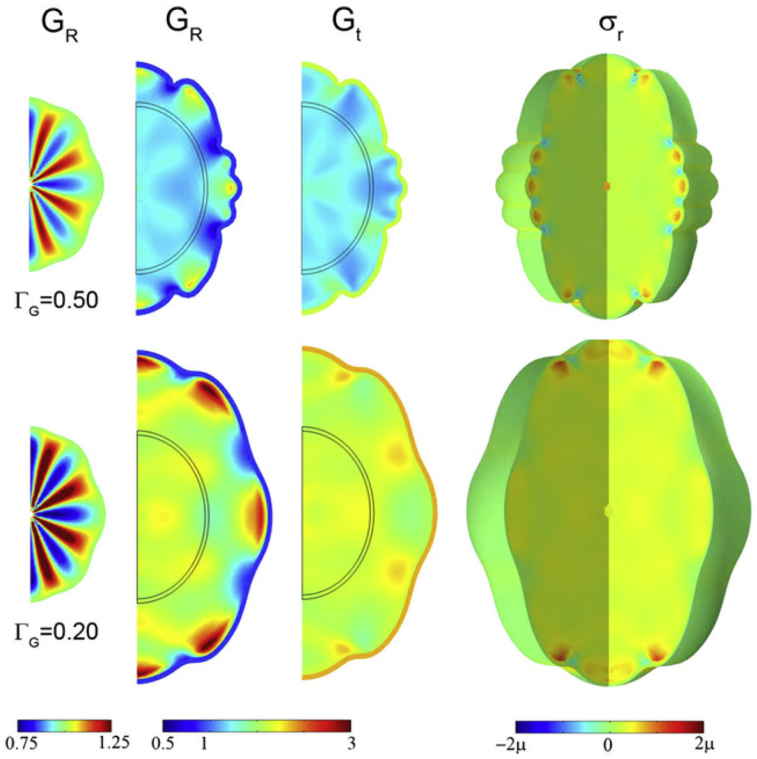

Fig. 12.

The effects of cortical growth rate and initial shape in an axisymmetric model of folding caused by tangential growth of the outer layer and stress-induced growth in internal regions. The initial shape (column 1) is determined by imposing a specific pattern of radial growth G_R before the period of rapid tangential expansion. The next three columns show maps of radial growth G_R; tangential growth G_t; and radial stress σ_r superimposed on the deformed domain. Two different relative growth rates lead to qualitatively different final shapes. Row 1: relative growth rate $\Gamma_G = 0.50$, at time $\tau = 0.90$. Row 2: $_G = 0.20$, at time $\tau = 1.25$. Reproduced with permission from Bayly et al. (2013).

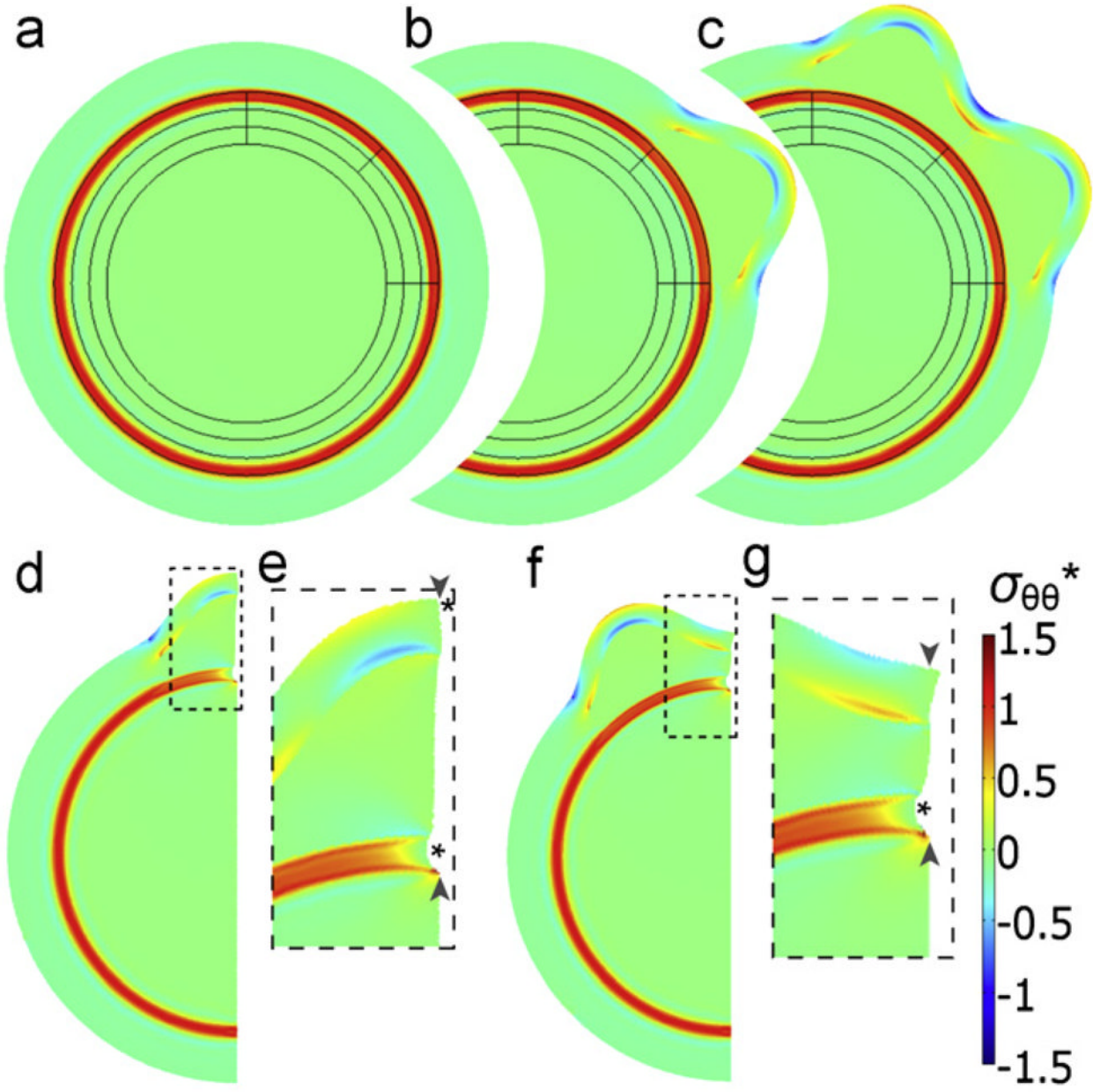

Fig. 13.

Two-dimensional finite element model of cortical folding caused by phased differential growth. In this model folding at specific locations is produced by spatial variations in the time of local expansion. (a)–(c) Model geometry and stress distribution (a) after contraction of a sub-cortical band of white matter, and before expansion of the outer cortical layer; and (b)–(c) after each of two local tangential expansions leading to the formation of two gyri. (d)–(g) A section of the model shown in (c) was used to simulate the effects of subsequent radial cuts within a gyrus (d and e) and a sulcus (f and g). Simulated cuts through the subcortical white matter tract (pairs of arrowheads) lead to openings (indicated by asterisks). Panels (e) and (g) are magnified images of the outlined regions in (d) and (f), respectively. Colors indicate circumferential stress (σ^*) normalized by the material shear modulus.

Reproduced with permission from Xu et al., (2010). (For interpretation of the references to color in this figure legend, the reader is referred to the web version of this article.)